Biogeosciences, 8, 289–300, 2011
www.biogeosciences.net/8/289/2011/
doi:10.5194/bg-8-289-2011

Biogeosciences

Influence of seasonal monsoons on net community production and CO_2 in subtropical Hong Kong coastal waters

X.-C. Yuan[1,2], K. Yin[3,4], W.-J. Cai[5], A. Y. Ho[2], J. Xu[2], and P. J. Harrison[2]

[1]Key Laboratory of Tropical Marine Environmental Dynamics, South China Sea Institute of Oceanology, Chinese Academy of Sciences, Guangzhou, China
[2]Division of Environment, Hong Kong University of Science and Technology, Clear Water Bay, Kowloon, Hong Kong, China
[3]School of Marine Sciences, Sun Yat-Sen University, Guangzhou, 510275, China
[4]Environmental Futures Centre, Griffith University, Brisbane, QLD 4111, Australia
[5]Department of Marine Sciences, the University of Georgia, Athens, Georgia 30602, USA

Received: 5 July 2010 – Published in Biogeosciences Discuss.: 19 July 2010
Revised: 24 January 2011 – Accepted: 24 January 201 – Published: 9 February 2011

Abstract. Data from seven cruises in three different environments including the Pearl River estuary, sewage discharge outfall, and eastern coastal/shelf waters were used to examine the seasonal variations in net community production (NCP) and the biologically active gases O_2 and CO_2. In the winter dry season, when monsoon-induced downwelling was dominant, NCP was negative ($-84 \pm 50\,\text{mmol C m}^{-2}\,\text{d}^{-1}$) in all three regions. The negative NCP corresponded to O_2 influxes of $100 \pm 50\,\text{mmol O}_2\,\text{m}^{-2}\,\text{d}^{-1}$ and CO_2 effluxes of $24 \pm 10\,\text{mmol C m}^{-2}\,\text{d}^{-1}$. In the summer wet season, when upwelling brought the deep oceanic waters to the coast due to the southwest monsoonal winds, there was a 2 to 15-fold increase in integrated primary production (IPP) compared to winter. The increase in IPP was likely due to the favorable conditions such as stratification and the nutrient inputs from upwelled waters and the Pearl River estuary. NCP in the mixed layer reached up to $110 \pm 48\,\text{mmol C m}^{-2}\,\text{d}^{-1}$ in the wet season. However, accompanying the high positive NCP, we observed an O_2 influx of $100 \pm 60\,\text{mmol O}_2\,\text{m}^{-2}\,\text{d}^{-1}$ and CO_2 efflux of $21 \pm 15\,\text{mmol C m}^{-2}\,\text{d}^{-1}$. The contradictory observation of positive NCP and CO_2 release and O_2 uptake in the mixed layer could be explained by the influence of the southwest monsoon-induced upwelling along with the influence of the Pearl River, as the upwelling brought cold, low dissolved oxygen (DO, $160 \pm 30\,\mu$M) and high dissolved inorganic carbon (DIC, $1960 \pm 100\,\mu$atm) water to the surface in the wet season. Hence, the subtropical Hong Kong coastal waters are generally a CO_2 source due to the monsoonal influence during both the dry-heterotrophic and wet-autotrophic seasons.

Correspondence to: K. Yin
(yinkd@mail.sysu.edu.cn)

1 Introduction

Urbanization and anthropogenic nutrients are known to result in eutrophication in many estuarine and coastal waters (Diaz and Rosenberg, 2008). The organic matter inputs from riverine outflow and domestic sewage effluent increase the occurrence of hypoxia or anoxia and result in high CO_2 release in some estuarine and coastal waters (Ducklow and McCallister, 2004; Diaz and Rosenberg, 2008; Borges et al., 2006), while the enhanced inorganic nutrient fluxes increase primary production and consequently oxygen production and the CO_2 sink (Mackenzie et al., 2004; Gypens et al., 2009). The ratio of dissolved inorganic nutrient to labile organic matter will determine how the CO_2 flux will be evolved (Gypens et al., 2009; Borges and Gypens, 2010).

Substantial attention has been paid to eutrophication impacts on biological activities (e.g. phytoplankton and bacteria), oxygen and CO_2 in temperate coastal and estuarine systems (Shiah and Ducklow, 1994; Borges et al., 2006), while subtropical coasts have been less well investigated. Many subtropical coastal waters are subjected to seasonal monsoons, northeast monsoonal winds in winter and the southwest monsoon in spring and summer, which considerably influenced biogeochemical cycling (Goyet et al., 1998; Mintrop et al., 1999; Yin, 2002, 2003). For example, in the Arabian Sea and northwestern Indian Ocean, seasonal

Published by Copernicus Publications on behalf of the European Geosciences Union.

variations in primary production and CO_2 release were closely associated with the influences of monsoons (Goyet et al., 1998; Mintrop et al., 1999; Lendt et al., 2003). Similarly, the subtropical coastal waters adjacent to the Pearl River estuary were also reported to be influenced by the seasonal monsoon. As a result of monsoonal effects, there are marked seasonal and temporal variations in nutrients and phytoplankton biomass in the coastal waters adjacent to the Pearl River estuary (Yin, 2002, 2003).

Hong Kong subtropical waters are located on the southern coast of China, facing the northwestern part of the South China Sea (SCS) and lying to the southeast of the Pearl River estuary. Hence, this region is an interface where the Pearl River estuary, sewage discharge outfall and oceanic water meet and interact, and consequently a potential zone for transferring high amounts of terrestrial carbon to the atmosphere and/or deeper ocean in the South China Sea. Coupled with the monsoonal influence, the seasonal freshwater discharge from the Pearl River further complicates the hydrodynamics and biochemical processes. Previous studies suggested that the anthropogenic inputs of nutrients and organic matter in the Pearl River estuary have led to a decrease in oxygen and an increase in CO_2, especially in the upper estuary (Yin et al., 2004; Cai et al., 2004; Dai et al., 2006). Zhai et al. (2005a) have reported that aerobic respiration is the most important process in maintaining a high $p$$CO_2$ level (>3000 µatm) in the upstream section of the Pearl River estuary. Being downstream of the Pearl River estuary, Hong Kong coastal waters have also been reported to be generally a CO_2 source due to the influence of the Pearl River discharge and sewage effluent (Yuan et al., 2010a). However, little is known about the seasonal variations in O_2 and CO_2 in response to monsoonal winds and the freshwater discharge of the Pearl River estuary.

In this study, several contrasting environments were studied: (1) western waters close to the Pearl River estuary; (2) Victoria Harbor – near a local sewage discharge outfall; and (3) eastern coastal/shelf waters – relatively far away from anthropogenic influences. By measuring the air-sea fluxes of O_2 and CO_2, primary production and dark community respiration (DCR) during seven cruises, we examined: (1) the influence of the Pearl River estuary and sewage discharge on O_2 and CO_2 dynamics; (2) the seasonal variations in biological metabolism (e.g. primary production and respiration), and (3) air-sea fluxes of O_2 and CO_2 in response to monsoonal winds.

2 Materials and methods

2.1 Study area and sampling

The annual average Pearl River discharge is 10 500 $m^3 s^{-1}$ with 20% occurring during the dry season in October to March and 80% during the wet season in April–September (Zhao, 1990). The river carries heavy pollution loads and high nutrient inputs into the western Hong Kong waters (Cai et al., 2004; Yin et al., 2004). In addition, Hong Kong waters receive >2 million tons of sewage effluent daily from the local sewage discharge in Victoria Harbor. In Hong Kong coastal waters, tides are predominantly semi-diurnal, and the mean tidal range is 1.7 m with a range from 1 m during neap tides to up to 2 m during spring tides with little seasonal tidal variation (Lee et al., 2006).

During 2005 and 2006, sampling was conducted at 8 stations (Fig. 1) at the surface (1 m), middle (4 m) and bottom (2 m above the bottom) in four seasons: winter (March 2006), spring (April 2006), summer (June 2005 and July 2005–2006) and fall (November 2005 and 2006). Based on nutrient concentrations and salinity, the 8 stations represent three main regions: Pearl River Estuary (S1–S2), Victoria Harbour (S3–S6), and Eastern Waters (S7–S8). Water samples were taken using a custom-made 5-L Plexiglas sampler. The vertical profiles of salinity and temperature were measured with a YSI® 6600 sensor. The mixed layer depth was determined as the first depth where the vertical change in seawater density was $\geq 0.2\,kg\,m^{-3}$ per meter (Therriault and Levasseur, 1985).

2.2 DO, dark community respiration (DCR) and primary production

Dissolved oxygen (DO) was determined in duplicate by Winkler titration, as outlined in the JGOFS protocols (Knap et al., 1994). After 4 to 5 volumes of water were allowed to overflow from the 60 ml BOD bottles, Winkler reagents were added. Winkler titrations were carried out in the laboratory with an automated titration apparatus (716 DMS Titrino, Metrohm®) that analyzed the samples with a potentiometric detector to determine the endpoint.

DCR (duplicate) was determined from the changes in DO in BOD bottles (60 ml) during a 24-h dark incubation period. The linearity of DO decrease over 24 h was verified in a separate time series experiment (Yuan et al., unpublished data, 2010). Samples were incubated in a water circulation tank simulating in situ temperature (±1 °C). For DCR, the average variation coefficient was 7 ± 5%, which was considered to be precise enough to measure respiration in coastal waters, although 5 replicates for respiration measurements have been recommended for oceanic waters where respiration is often $<3\,\mu M\,d^{-1}$ (Robinson and Williams, 2005).

Seawater samples for the primary production measurements were pre-screened through a 200 µm mesh net, and then a 50 ml sample was transferred to acid-washed glass tubes to which 0.4–2 µCi (14.8–74 kBq) of ^{14}C-labelled sodium bicarbonate ($NaH^{14}CO_3$) was added (see details in Ho et al., 2010). Duplicate tubes were wrapped with different layers of screening to provide light fields corresponding to approximately 100, 55, 30, 10, and 1% of surface irradiance. Samples were incubated for 4 h on-deck in running

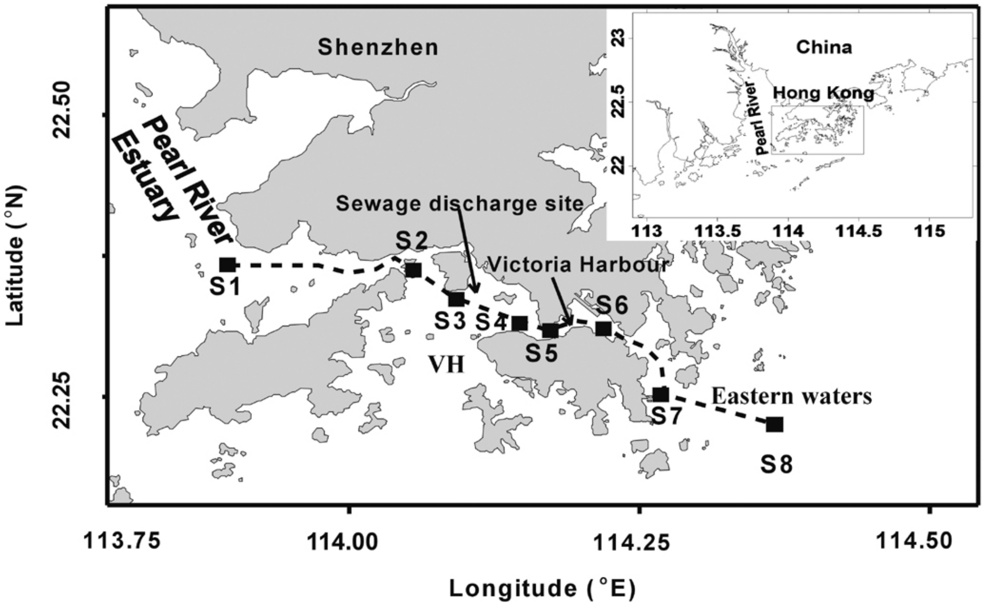

Fig. 1. Map and sampling stations along a transect from S1 near the Pearl River estuary to S8 in eastern coastal/shelf waters. The sewage discharge site is located between S3 and S4.

surface seawater. The incubation was terminated after 4 h by filtering sequentially through a GF/F filter (∼0.7 µm nominal pore size). Filters were put into a scintillation vial, and HCl (0.25 ml, 0.1 N) was added to the scintillation vials to remove the inorganic $NaH^{14}CO_3$. Counting was carried out using a liquid scintillation counter (LKB Rack Beta). Primary productivity at each depth was calculated according to Jassby and Platt (1976). Daily primary production was estimated by multiplying the ratio of the whole day's irradiance to the irradiance during the incubation period, in order to minimize the bias caused by differences in irradiance for the incubations conducted at the different times of the day. The respiration of ^{14}C labeled organic matter, which partially depends on the incubation time (Gazeau et al., 2007), and the ^{14}C uptake rates were assumed to be representative of gross primary production with an insignificant amount of respiration of ^{14}C labeled organic matter due to the short incubation time (4 h) in this study. Net community production (NCP) was calculated by gross primary production minus dark community respiration. The integrated gross primary production (IPP), dark community respiration (IDCR) and NCP was calculated by averaging the measured production between two depths and multiplying by the depth interval in the mixed layer depth (Ichimura et al., 1980). Carbon and O_2 units were converted using the Redfield ratio of 106C:138O.

2.3 DIC and $p\mathrm{CO_2}$

Water samples (50 ml) were preserved with saturated $HgCl_2$ (20 µ l) for dissolved inorganic carbon (DIC) analysis and stored in a cool dark chamber at 4 °C. DIC was measured within 1 week by acidification and subsequent quantification of CO_2 with an Infra-red (IR) detector (Li-Cor 6252) using a DIC analyzer (AS-C2, Apollo SciTech). This method has a precision of 0.1 to 0.2% in coastal water (Cai and Wang, 1998). DIC was calibrated against Certified Reference Material from A. Dickson, Scripps Institution of Oceanography, and a duplicate analysis was made every tenth sample (Dickson and Goyet, 1994). pH was measured with an Orion Ross combination glass electrode (Dickson and Goyet, 1994). We used three NBS pH buffers (pH = 4, 7, and 10) to calibrate the pH electrode slopes and a 2-amino-2-hydroxymethyl-1,3-propanediol (tris) buffer at salinity 35 to derive a pH scale based on total proton concentration (Dickson and Goyet, 1994). $p\mathrm{CO_2}$ was calculated from measured pH values and DIC concentrations for estuarine and coastal waters using the following equation (Cai and Wang, 1998):

$$p\mathrm{CO_2} = \frac{[\mathrm{CO_2}]}{K_H} = \frac{C_T\{H\}^2}{(\{H\}^2 + \{H\}K_1 + K_1K_2)K_H} \tag{1}$$

where C_T is the DIC value, $\{H\}$=$10^{-\mathrm{pH}}$, K_H is the solubility constant (Weiss, 1974), and K_1 and K_2 are the constants for carbonic acid (Roy et al., 1993). A maximum error of 0.01 pH units (in total scale) will result in an uncertainty of ±3% in $p\mathrm{CO_2}$ (ca. 15 ± 6 µatm CO_2). Due to the high $p\mathrm{CO_2}$ in Hong Kong waters, the error introduced by this term (ca. ±10% or 3 ± 2 mmol C m^{-2} d^{-1}) should not affect our conclusion.

2.4 Air-sea fluxes of CO_2 and O_2

The CO_2 and O_2 fluxes across the air-sea interface are calculated by following the one-dimensional stagnant-film model:

$$CO_2 \text{ flux} = k_{CO_2} \quad \beta(pCO_{2w} - pCO_{2a}) \tag{2}$$

$$O_2 \text{ flux} = k_{O_2}([O_2] - [O_2]_S) \tag{3}$$

where k_{CO_2} and k_{O_2} are the gas transfer velocities for CO_2 and O_2, respectively; β (Bunsen coefficient) is the solubility of CO_2 at a given temperature and salinity. The CO_2 solubility coefficient was obtained from Weiss (1974). pCO_{2w} and pCO_{2a} represent the partial pressure of CO_2 in surface water and overlying air, respectively. k_{CO_2} was calculated according to Wanninkhof (1992) as follows:

$$k_{CO_2} = f \times u_{10}^2 \times (Sc/660)^{-0.5} \tag{4}$$

where f is a proportionality factor (0.31), u_{10} is the wind speed at 10 m height, *Sc* is the Schmidt number of CO_2 in seawater and 660 is the *Sc* value in seawater at 20 °C. $[O_2]$ and $[O_2]_S$ represent the measured concentrations and estimated oxygen solubility, respectively. DO solubility was calculated according to Benson and Krause (1984). The calculation of k_{O_2} is similar to k_{CO_2} except the Schmidt number for O_2 was used (Wanninkhof, 1992). Daily wind speed at 10 m was obtained from the Hong Kong observatory (http://www.weather.gov.hk/).

The atmospheric pCO_2 has been reported to be in the range of 349 to 372 µatm in inner shelf/coastal areas adjacent to the Pearl River plume (Zhai et al., 2005a), and ∼358 µatm in offshore waters (Zhai et al., 2009). Since our sampling sites are very close to a mega city (Hong Kong), the influence of land mass may result in a high atmospheric pCO_2, especially in the dry season when northeast winds were dominant. A large range in the atmospheric pCO_2 (349 to 460 µatm, and averaged 400 µatm) was reported in Randers Fjord, Scheldt, and the Thames (Borges et al., 2004), where sampling sites were also close to anthropogenic influences. Furthermore, atmospheric CO_2 was estimated to be ∼370 to 390 µatm at a nearby location (23° N, 120° E) during 2006 based on data from the NOAA data archive center (http://www.esrl.noaa.gov/gmd/ccgg/globalview/). The variations in atmospheric pCO_2 (370 to 390 µatm) would quantitatively result in an estimate of average CO_2 effluxes of 20 mmol C m^{-2} d^{-1} with variations from 16 to 22 mmol C m^{-2} d^{-1}. While the lack of the precisely known atmospheric CO_2 level has caused the largest uncertainty for our CO_2 flux estimate, it does not invalid our conclusions regarding important mechanisms controlling metabolic states and O_2 and CO_2 fluxes in this type of coastal water.

2.5 Nutrients

Samples for nutrients were taken with a 60 ml syringe and filtered through a pre-combusted Whatman GF/F filter mounted in a Swinnex filter holder and dispersed into Nalgene bottles. All plastic-ware was pre-cleaned with 10% HCl. The filtered nutrient samples were placed in a cooler with dry ice and then frozen in the laboratory until analyzed. Nutrients (nitrate, ammonium and phosphate) were measured with a Skalar San autoanalyzer following JGOFS protocols (Knap et al., 1994).

2.6 Statistical analyses and calculations

The difference in seasonal and spatial variations in DO and CO_2 was assessed using an analysis of variance followed by a means comparison (t-test). The error bars for the bioassay represent a pooled sample standard deviation of the means. The Pearson test was used to obtain the correlation coefficient and the significance of the correlation. A significance level of 0.05 was used to determine statistical differences. All statistical analyses were performed using SPSS statistical software (SPSS Inc.).

Data on salinity, temperature, primary production, DO, DIC and pCO_2 at stations 1 to 8 were presented in Ho et al. (2008 and 2010) and Yuan et al. (2010a). In this study, these data along with wind, respiration and gaseous air-sea fluxes were grouped into three main regions (Pearl River estuary, Victoria Harbor and eastern waters) and two seasonal patterns. The average values of all seasonal parameters (e.g. salinity, temperature, primary production and DIC etc.) were calculated by averaging data from April to October for the wet season, and November to March for the dry season.

3 Results

3.1 Seasonal variations in salinity, temperature and nutrients

Surface water salinity exhibited a clear seasonal variation due to the seasonal freshwater discharge from the Pearl River. Surface salinity was high (∼33) in the dry season (October to March) in all three regions, and reached a minimum (15–31) in summer (Figs. 2 and 3). Spatially, surface salinity was not significantly different between the regions in the winter dry season ($p > 0.05$), but increased from ∼15 near the Pearl River estuary to ∼31 in eastern waters in the spring and summer wet season, indicating a strong influence of freshwater discharge from the Pearl River estuary ($p < 0.05$) (Figs. 2 and 3). Surface water temperature also varied seasonally, ranging from ∼18 °C in the dry season to ∼27 °C in the wet season at all stations (Figs. 2 and 3).

Vertically, salinity at the surface and bottom were not significantly different in the winter dry season indicating strong vertical mixing ($p > 0.05$), while strong stratification was present in the summer wet season (Fig. 3). In the wet season, the stratified depths decreased from 6 m near the Pearl River estuary to ∼2 m in eastern waters (Fig. 3), suggesting strong upwelling effects and less influence of freshwater discharge in eastern waters. In addition, dissolved inorganic

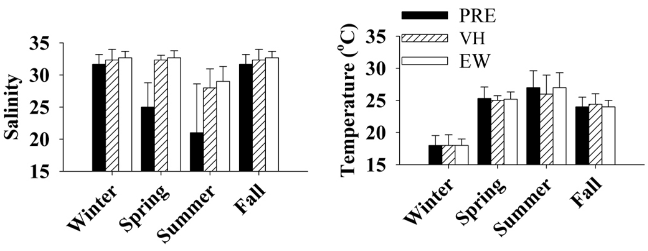

Fig. 2. Seasonal average surface salinity and temperature at S1 to S2 (Pearl River estuary, PRE), S3 to S6 (Victoria Harbor, VH) and S7 to S8 (eastern waters, EW) during 2005 and 2006. Salinity and temperature data are obtained from Hong Kong Environmental Protection Department. Error bars = ±1 SD and $n = 4$ to 12.

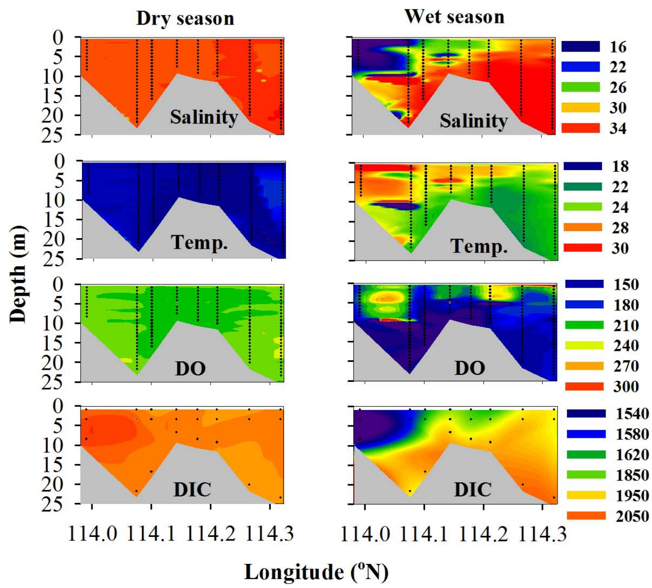

Fig. 3. Vertical contour of salinity, temperature (°C), dissolved oxygen (µM) and dissolved inorganic carbon (DIC, µM) from S1 near the Pearl River estuary to S8 in eastern coastal/shelf waters in **(A)** the winter dry season (March 2006) and **(B)** the summer wet season (July 2006).

nitrogen (DIN) concentrations increased ~2-fold in the wet season (Table 1).

3.2 DO, DIC and air-sea fluxes of O_2 and CO_2

There were no significant seasonal variations in surface DO concentrations in all regions ($p > 0.05$) (Fig. 4a). Lower surface DO concentrations (180–220 µM) were usually found in Victoria Harbor near the sewage discharge outfall (Fig. 4a). In contrast, bottom DO concentrations exhibited a clear seasonal variation, which decreased from 210–230 µM in the dry season to 150–210 µM in the summer wet season ($p < 0.05$) (Fig. 3).

Surface water oxygen was generally undersaturated and thus there was an O_2 influx from the atmosphere in all regions (Fig. 4b). Influx of O_2 exhibited no significant difference between the wet and dry seasons ($p > 0.05$), but it was spatially variable with the low influx in eastern waters (14 ± 90 mmol O_2 m^{-2} d^{-1}) and high in Victoria Harbor (100 ± 120 mmol O_2 m^{-2} d^{-1}) (Fig. 4b).

Similar to salinity, DIC concentrations were vertically homogenous in the dry season, but became stratified in the wet season (Fig. 3). Surface pCO_2 exhibited a seasonal variation near the Pearl River estuary, with higher pCO_2 in the spring and summer wet season (800 ± 100) than in the dry season (500 ± 90 µatm) ($p < 0.05$) (Fig. 4c). However, pCO_2 did not exhibit significant seasonal variations in the other two regions ($p > 0.05$) (Fig. 4). CO_2 effluxes were higher near the Pearl River estuary and Victoria Harbor (26 ± 20 mmol C m^{-2} d^{-1}) and decreased to 6 ± 5 mmol C m^{-2} d^{-1} in eastern waters (Fig. 4d) ($p < 0.05$). Similarly, O_2 influxes were higher near the Pearl River estuary and Victoria Harbor (150 ± 40 mmol C m^{-2} d^{-1}) and decreased to 20 ± 10 mmol C m^{-2} d^{-1} in eastern waters (Fig. 4d) ($p < 0.05$).

3.3 DCR and NCP

In mixed layer, IPP was lower (20–100 mmol C m^{-2} d^{-1}) in winter than summer (40–200 mmol C m^{-2} d^{-1}) in Hong Kong waters ($p < 0.05$) (Fig. 6). The NCP also exhibited seasonal and spatial variations. A seasonal comparison revealed that NCP in the mixed layer was negative (~ -80 mmol C m^{-2} d^{-1}) in winter, positive (up to 110 mmol C m^{-2} d^{-1}) in summer, and in between in spring (-10 to 40 mmol C m^{-2} d^{-1}) (Fig. 5a). Due to the shallower mixed layer depth, IDCR was lower in summer wet season in comparison with the dry season (Fig. 5b). In general, NCP was positive in the wet season, while negative in the dry season (Fig. 5b), indicating that Hong Kong waters shifted from autotrophy in the wet season to heterotrophy in the dry season.

4 Discussion

4.1 Influence of the Pearl River discharge and sewage effluent

Hong Kong waters are influenced by the summer Pearl River discharge in the western waters, and year-round domestic sewage effluent in Victoria Harbor. The significant correlation between pCO_2 and salinity suggested an important influence of the Pearl River estuary ($p < 0.05$, Table 2). Surprisingly, there was no significant correlation between pCO_2 and surface temperature ($p > 0.05$, Table 2). Although

Table 1. Seasonal variations in depth (m), photic depth (1% light depth) (PD, m), mixing layer depth (MLD, m), integrated dark community respiration (IDCR, mmol C m^{-2} d^{-1}), net community production (NCP, mmol C m^{-2} d^{-1}) and air-sea CO_2 flux (F_{CO_2}, mmol C m^{-2} d^{-1}) in the mixed layer, surface and bottom salinity (S_s and S_b), temperature (T_s and T_b, °C), dissolved inorganic nitrogen (DIN_s and DIN_b, µM) and dissolved inorganic carbon (DIC_s and DIC_b, µM) near the Pearl River estuary (PRE), Victoria Harbour (VH) and eastern waters (EW) (see Fig. 1 for locations). ±1 SD and $n = 2$ to 9.

	Winter			Spring			Summer			Fall		
	PRE	VH	EW	PRE	VH	EW	PRE	VH	EW	PRE	VH	EW
Depth	20	12	27	20	12	27	20	12	27	20	12	27
PD	7	10.5	24	10	8.5	17.5	7	11	12	9	8.7	15
MLD	18	12	20	6	7.5	8	6	4	2	7	12	22
IDCR	165 ±25	124 ±60	154 ±40	113 ±5	93 ±5	34 ±20	60 ±18	30 ±10	50 ±70	142 ±13	136 ±20	140 ±12
NCP	−144 ±20	−98 ±38	−54 ±45	36 ±42	−12 ±30	26 ±10	40 ±10	80 ±30	110 ±48	−25 ±56	−86 ±6	−96 ±41
F_{CO_2}	22 ±5	31 ±5	8 ±3	32 ±3	19 ±4	4 ±3	43 ±8	27 ±9	4 ±16	20 ±1	35 ±2	7 ±14
S_s	32	32	33	25	32	33	21	28	29	32	32	33
S_b	33	33	33	32	34	34	32	33	34	33	33	34
T_s	18	18	18	25	24	24	26	25	25	27	27	26
T_b	18	18	17	24	23	23	24	23	22	25	25	25
DIN_s	16	11	7	26	20	8	26	23	14	31	32	16
DIN_b	15	11	7	23	21	7	23	18	8	28	26	12
DIC_s	2011	1999	1989	1887	1940	1943	1789	1844	1850	1956	1921	1930
DIC_b	2011	1999	1989	1940	1957	1951	1907	1947	1969	1956	1955	1958

temperature variations often regulate pCO_2 (Borges et al., 2005), many other factors (e.g. high NCP, lateral and vertical mixing) masked the relationship between temperature and pCO_2 in Hong Kong waters.

Hong Kong waters receive large amounts of inorganic nutrients, DIC, and terrestrial organic matter from the Pearl River and sewage discharge. NH_4 is a good indicator of sewage impacts (Yin and Harrison, 2007), and it significantly correlated with pCO_2 in Victoria Harbor (Table 2). There was no significant correlation between pCO_2 and NO_3 concentrations (Table 2), which was likely due to the fact that NO_3 was the least preferred N source based on ^{15}N uptake rates compared to NH_4 (Yuan et al., unpublished data, 2010). The high inputs of N from the Pearl River resulted in a high N/P ratio (∼40) in spring and summer (Table 1), which consequently caused phosphorus limitation for phytoplankton growth (Yin, 2002), and for bacterial respiration (BR) in the wet season in southern Hong Kong waters (Yuan et al., 2010b). Dissolved organic carbon (DOC) also increased to 200 µM in Victoria Harbor in both the dry and wet seasons (Yuan et al., unpublished data, 2010). Hence, the increase in inorganic nutrients and organic carbon not only increased primary production in summer (Ho et al., 2010), but also produced an increase in bacterial production (BP) and BR (Yuan et al., 2010a).

Total alkalinity (TA) fluxes into the South China Sea were estimated to be 462×10^9 mol y^{-1} from the Pearl River, but the DIC/TA in the Pearl River is very close to 1 (Guo et al., 2008), thus it should not have significant impact on the pCO_2 variation in the Hong Kong waters. A high input of alkalinity could lead to an elevated TA/DIC ratio and result in the formation of a significant CO_2 sink, such as in the Yellow Sea Water (Chou et al., 2009a). Anaerobic alkalinity generation in sediments could enhance alkalinity in coastal waters (Thomas et al., 2009), but anaerobic activities are rare in Hong Kong waters due to the absence of hypoxia. Therefore, the effects of anthropogenic alkalinity inputs (e.g. sewage discharge) on CO_2 variation need further investigation in Hong Kong waters.

Coupled with the biochemical variations, physical factors are very important in Hong Kong waters. The high freshwater input from the Pearl River discharge in western waters increased the horizontal flushing and reduced water residence time since 80% of the discharge occurs during the wet season in April–September (Zhao, 1990; Yin, 2002). The residence time is much shorter (∼1.5 to 2.5 days) in the wet season, and hence there is strong horizontal advection (Kuang and Lee, 2004). Therefore, abnormally low or high oxygen waters caused by high phytoplankton production or BR could be replaced quickly by a water mass from the Pearl River estuary and bottom oceanic waters due to the short residence

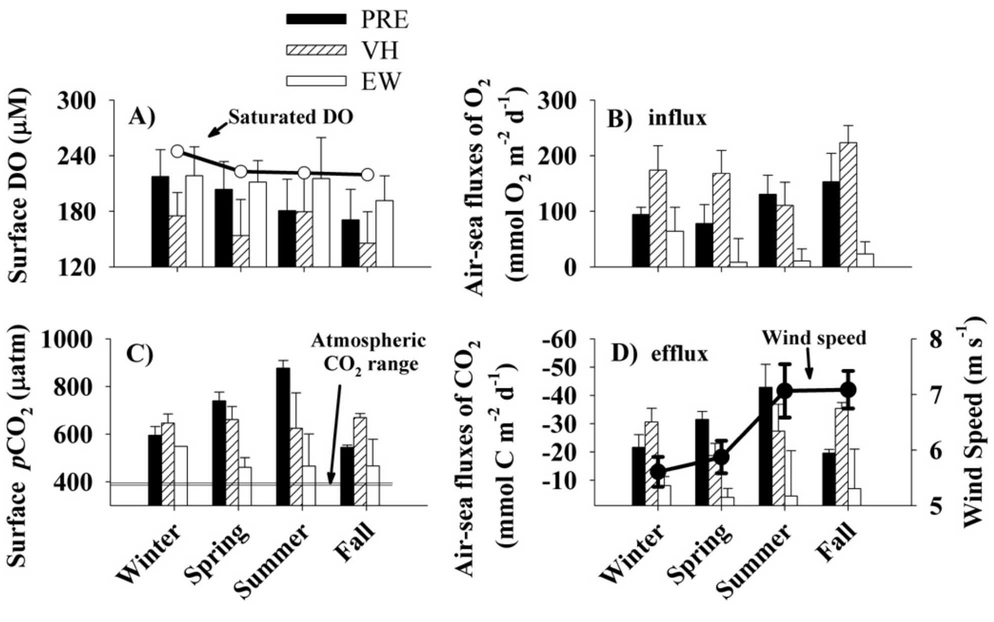

Fig. 4. Seasonal variations in **(A)** surface DO, **(B)** air-sea fluxes of O_2, **(C)** surface pCO_2 and **(D)** air-sea fluxes of CO_2 near the Pearl River estuary (PRE), Victoria Harbor (VH) and eastern coastal/shelf waters (EW) during 2005 and 2006. Error bars = ±1 SD and $n = 4$ to 12. The saturated DO, wind speed and a range of atmospheric pCO_2 levels (349 to 460 µatm) are indicated.

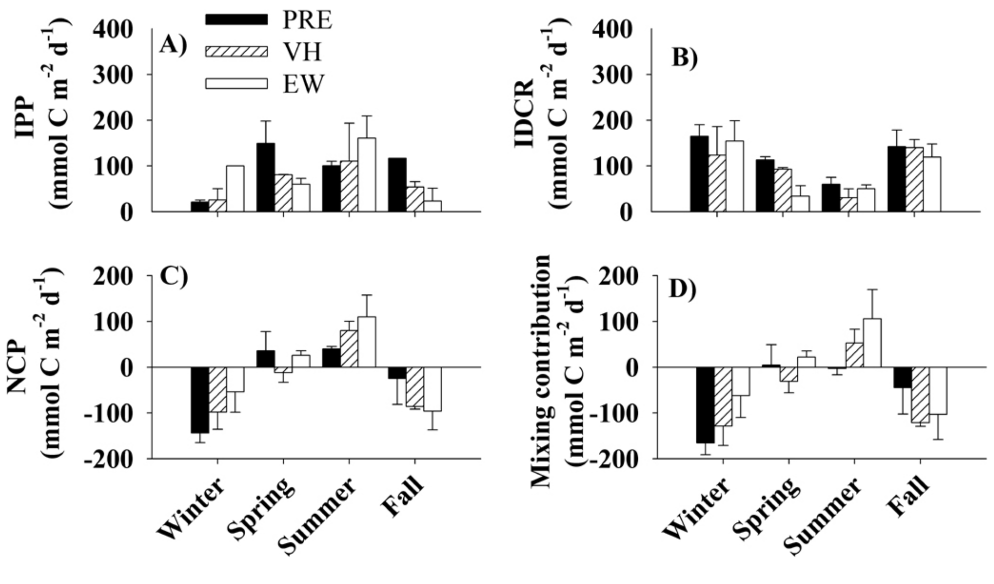

Fig. 5. Seasonal variations in **(A)** integrated primary production (IPP), **(B)** dark community respiration (DCR), **(C)** net community production (NCP) and **(D)** mixing contribution to CO_2 in the mixed layer during 2005 and 2006. IPP data were obtained from Ho et al. (2010). Error bars = ±1 SD and $n = 4$ to 12.

time. Harrison et al. (2008) concluded that there is no massive hypoxia in the lower Pearl River estuary due to a short residence time of the seawater. Hence, the eutrophication impact in Hong Kong waters was not as severe as expected for such a eutrophic area in the wet season (Ho et al., 2008; Yuan et al., 2010a), as DO remained >150 µM with solubility ranging from 210 to 240 µM (Fig. 4a).

4.2 O_2 and CO_2 in relation to trophic status

The CO_2 efflux varied from 3 mmol C m^{-2} d^{-1}in eastern waters to 40 mmol C m^{-2} d^{-1} near the Pearl River estuary (Fig. 4), which were of the same magnitude as inner/coastal shelf waters measured by Zhai et al. (2005b). The slope of the regression between the air-sea fluxes of CO_2 and O_2 indicated that O_2 flux was ~7-fold faster than CO_2 (data not

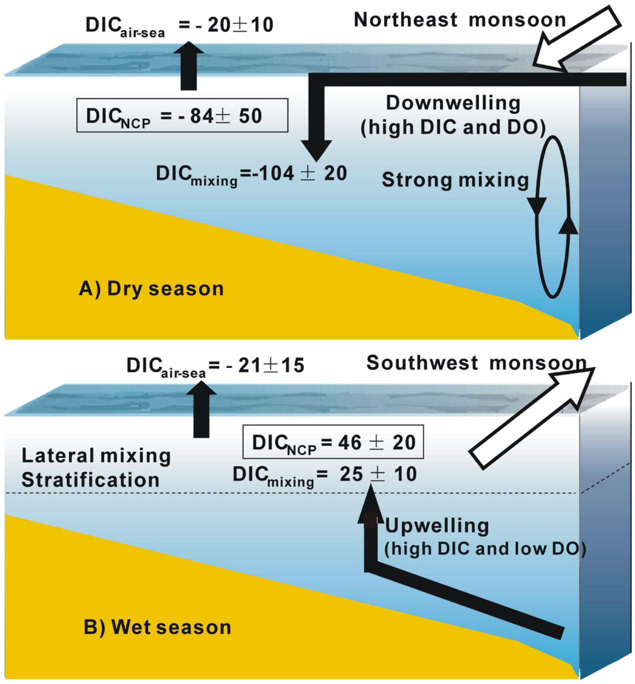

Fig. 6. A conceptual carbon transport model and a mass balance analysis in the **(A)** dry and **(B)** wet seasons. Units are in $\mathrm{mmol\,C\,m^{-2}\,d^{-1}}$. DIC_{mixing} is the mixing contribution to DIC variations; $DIC_{air\text{-}sea}$ is air-sea CO_2 exchange; DIC_{NCP} is the integrated net community production in the mixed layer, which were estimated with overall average in the three regions (the Pearl River estuary, Victoria Harbor and EW), respectively. Negative values represent CO_2 losses and positive values are CO_2 releases into water column, but positive NCP corresponds to CO_2 loss. Error bars $= \pm 1$ SD and $n = 14$ to 21.

shown). Carrillo et al. (2004) reported that oxygen concentrations approached atmospheric equilibrium much faster than CO_2 during the same time span, suggesting that O_2 flux was ~8.3-fold faster than CO_2. Zhai et al. (2009) also reported that O_2 approaches equilibrium with the atmosphere much faster than the CO_2 in the northern South China Sea.

An important question concerning the Hong Kong estuarine ecosystem functionality is whether it is autotrophic or heterotrophic. Our results indicated that O_2 influxes and CO_2 effluxes might not always be a good indicator of heterotrophy or autotrophy (i.e. production vs. respiration) in the Hong Kong coastal waters. Interestingly, while NCP negatively correlated with pCO_2 in Victoria Harbor and eastern waters, NCP and chl-*a* positively correlated with pCO_2 in the Pearl River estuary (Table 2). Hence, although high positive NCP reduced DIC, pCO_2 did not always negatively correlate with NCP due to the presence of other processes (e.g. due to input of high pCO_2 deep water via upwelling and lateral transport from the Pearl River estuary). Borges et al. (2006) reported that a positive NCP was associated to a source of CO_2 during a cruise in the Bay of Palma, when NCP values are integrated throughout the water column. They further confirmed that if the CO_2 fluxes are compared to NCP in the mixed layer, then there is an agreement between the direction of the CO_2 fluxes and the trophic status (Borges et al., 2006). In addition, Chou et al. (2009b) reported that heterotrophic waters act as a significant CO_2 sink in summer in the East China Sea (ECS) shelf, because waters are undersaturated with respect to atmospheric CO_2 above the pycnocline (~10 to 30 m), but supersaturated with CO_2 below the pycnocline. In contrast to their observations, our results showed a contradictory phenomenon in which positive NCP coincided with a CO_2 source and O_2 sink in the mixed layer in the wet season (Fig. 6).

4.3 Monsoonal influences

We now offer an explanation for the apparently inconsistent observations of positive NCP and the ingassing of O_2 and degassing of CO_2. We suggest that a more important regulatory factor of O_2 and CO_2 fluxes is the physical mixing such as downwelling and upwelling due to seasonal monsoons, along with the lateral mixing of riverine waters. The strong seasonal changes in salinity, temperature, chl-*a* and nutrients have been reported to be closely coupled with seasonal monsoons (Yin, 2002, 2003). The responses of O_2 and CO_2 fluxes to the seasonal monsoons have not been addressed in previous studies in Hong Kong waters, although the monsoonal influence on CO_2 has been studied in a tropical estuarine system off Goa, India (Sarma et al., 2001).

In the winter dry season, prevailing northeastern monsoonal winds cause downwelling due to the Ekman transport, and the downwelling results in the shoreward movement of surface offshore waters (Yin, 2002, 2003). Hence the Pearl River estuary and the adjacent coastal waters are dominated by offshore waters which results in low temperature, nutrients, chl-*a* and high salinity (Yin, 2002, 2003). In the summer wet season, surface waters flow offshore (southwards) due to the southwest monsoon-induced winds which draw the bottom oceanic waters from the continental shelf to the nearshore, and hence high salinity and low temperature were present at the bottom (Fig. 3).

Similarly, monsoonal influence and the freshwater discharge from the Pearl River estuary also exerted important influences on NCP. As described in the conceptual carbon transport model (Fig. 6), cold offshore water moves shoreward with high DIC and DO in the winter dry season. Light availability was reduced due to strong vertical mixing (Ho et al., 2010), which resulted in a negative NCP ($-84 \pm 50\,\mathrm{mmol\,C\,m^{-2}\,d^{-1}}$) in all three areas (Fig. 6). Accompanying the negative NCP, there was a CO_2 efflux ($21 \pm 10\,\mathrm{mmol\,C\,m^{-2}\,d^{-1}}$) (Fig. 4). In the spring and summer wet season, the freshwater input increased nutrient availability and resulted in stratification at the surface (Yin, 2002, 2003). Due to high nutrient inputs from the Pearl River estuary, IPP increased by 2 to 15-fold in summer in

Table 2. Step-wise regression analysis performed for each region separately. pCO_2 is the dependent variable (y axis). Sea surface salinity (SSS), temperature (SST), Chl-*a*, NO_3, NH_4, PO_4 and net community production (NCP) is the independent variable, respectively. Slope is not presented when significant value $p > 0.05$. $n = 14$ to 25.

	PRE			VH			EW		
	Slope	r^2	p	Slope	r^2	p	Slope	r^2	p
SSS	−21	0.5	0.01	−21	0.3	0.02	−8	0.3	0.05
SST	–	–	–	–	–	–	–	–	–
Chl-*a*	14	0.3	0.05	−23	0.3	0.05	−13	0.3	0.05
NO_3	–	–	–	–	–	–	–	–	–
NH_4	−24	0.4	0.02	5	0.6	0.01	–	–	–
PO_4	280	0.3	0.05	142	0.4	0.02	−80	0.3	0.05
NCP	0.18	0.3	0.05	−12	0.3	0.05	−0.22	0.5	0.01

Table 3. Surface and bottom DIC (DIC_s and DIC_b), difference between DIC_s and DIC_b (DIC_{b-s}), surface net community production (NCP) in the mixed layer (note that unit of NCP was converted to $\mu M\,d^{-1}$), and NCP: DIC_{b-s} ratios (%) in summer during 2005 and 2006, respectively.

		2005			2006		
	Units	PRE	VH	EW	PRE	VH	EW
DIC_s	µM	1864	1857	1860	1713	1830	1940
DIC_b	µM	1958	1962	1951	1856	1932	1956
DIC_{b-s}	µM	94	95	91	143	82	16
NCP	$\mu M\,d^{-1}$	27 ±10	46 ±30	12 ±48	32 ±42	72 ±30	100 ±10
NCP:DIC_{s-b}	%	29	48	13	22	88	600

comparison with winter (Fig. 5). However, in comparison with the dry season, the air-sea flux directions of O_2 and CO_2 did not change, and O_2 influxes and CO_2 effluxes were $100\,mmol\,O_2\,m^{-2}\,d^{-1}$ and $21\,mmol\,C\,m^{-2}\,d^{-1}$ respectively in the wet season, although the high positive NCP showed a net biological CO_2 uptake (Figs. 4 and 6). In addition, the moderate DO (160 ± 30 µM) and high DIC (1960 ± 100 µM) in upwelled waters would offset an increase in DO and decrease in CO_2 by high phytoplankton photosynthesis (Figs. 3 and 6). Therefore, surface DO, pCO_2 and their air-sea fluxes fluctuated with much less seasonality, in contrast to salinity, temperature and IPP ($p < 0.05$) (Figs. 2, 4 and 6).

In order to quantify the contributions of the physical mixing, we conducted a mass balance analysis of DIC. The DIC concentrations reflect a balance between the influence of the mixing of the Pearl River and offshore waters, degassing to the atmosphere and net internal biological production which could be expressed approximately as:

$$DIC_{t2-t1} = DIC_{mixing} + DIC_{air\text{-}sea} + DIC_{NCP} \quad (5)$$

where DIC_{t2-t1} is the DIC difference from time 1 ($T1$) to time 2 ($T2$); DIC_{mixing} is the DIC change caused by physical mixing (both vertically and laterally); $DIC_{air\text{-}sea}$ is the DIC change caused by the air-sea exchange of CO_2; DIC_{NCP} is the DIC change caused by NCP. The mixing contribution to DIC was seasonally variable as the mixing reduced DIC in the dry season and increased it in the wet season (Fig. 5d). Overall, the mixing contribution to CO_2 in Hong Kong waters was $-104\,mmol\,C\,m^{-2}\,d^{-1}$ in the dry season and $25\,mmol\,C\,m^{-2}\,d^{-1}$ in the wet season (Fig. 6). The upwelling would increase DIC, whereas lateral mixing with freshwater with lower DIC from the Pearl River estuary might decrease DIC. Hence, the positive mixing contribution to CO_2 in the wet season suggested that DIC concentrations increased due to the net effects of upwelling and lateral mixing (Fig. 6). The difference between the surface and bottom DIC was often higher than NCP (Table 3), showing that bottom DIC could potentially supply enough DIC for high biological uptake (i.e. NCP) at the surface during upwelling period.

Contributions of lateral mixing and upwelling to the water masses were estimated using the following equation:

$$S_{EW} = S_{PRE} \times P_{PRE} + S_B \times (1 - P_{PRE}) \quad (6)$$

where S_{EW} and S_{PRE} are the surface salinities in eastern waters and Pearl River estuary respectively, and S_B is the bottom oceanic salinity in eastern waters (see salinity data in Table 1). P_{PRE} is the proportion of the water masses from the Pearl River estuary. Hence, it is estimated that 20 to 50% of the surface water masses in Victoria Harbor and eastern waters came from the water mass from the Pearl River estuary in the wet season, while 50 to 80% came from oceanic waters in the wet season.

4.4 Global relevance

In Hong Kong waters, the average NCP in the wet season was positive in both the mixed layer (46 mmol C m^{-2} d^{-1}) and the whole photic zone (240 mmol C m^{-2} d^{-1}), while Hong Kong coastal waters are sources of atmospheric CO_2. Hence, our observation suggested that the trophic state was not always a determinant factor on the direction of the air-sea CO_2 flux.

On a global scale, Longhurst et al. (1995) have reported their estimates of global coastal net ecosystem production to be 32.1 mol C m^{-2} y^{-1}, and Gattuso et al. (1998) estimated coastal gross primary production to be 17.4 mol C m^{-2} y^{-1}. However, worldwide measurements of $p\mathrm{CO_2}$ indicate that most inner estuaries and near-shore coastal areas are over-saturated with respect to atmospheric CO_2 (Borges et al., 2005; Cai et al., 2006; Chen and Borges, 2009; Laruelle et al., 2010). Hence, positive global coastal net ecosystem production is also associated with a source of atmospheric CO_2.

In terms of CO_2 (or O_2) sink and source, monsoon-induced upwelling is a "double-edged sword" in monsoon influenced waters. Some previous studies showed that upwelled nutrients indirectly decreased $p\mathrm{CO_2}$ by providing a source of new nutrients for photosynthesis in the upwelling system off the Galician coast (Borges and Frankignoulle, 2002). In the northern South China Sea, Zhai et al. (2009) also observed that there was biological drawdown of $p\mathrm{CO_2}$, which resulted in a CO_2 sink in coastal upwelling areas near Hainan Island in July 2004. The studies in the Arabian Sea suggested that CO_2 degasses into the atmosphere due to coastal upwelling, by bringing cold and CO_2-rich deep water to the surface, where NCP increases considerably during the southwest monsoon compared to northeast monsoon (Goyet et al., 1998; Barber et al., 2001; Dickson et al., 2001; Lendt et al., 2003).

Takahashi et al. (2002) have concluded that, because most of the upwelling occurs in low latitudes, these regions tend to be CO_2 source areas, whereas high latitudes are sink regions of CO_2 uptake. In addition, the global synthesis by Borges (2011) indicated that coastal upwelling areas with oxygen minimum zones (OMZ) are sources of atmospheric CO_2 in areas such as the Arabian Sea and the Peruvian and Chilean coasts, while coastal upwelling areas devoid of an OMZ or with deep OMZs are sinks for atmospheric CO_2 such as the Iberian and Oregon coasts. Hence, the seawater circulation and chemical properties complicate the relationship between the CO_2 and trophic status.

5 Conclusions

In this study, we simultaneously estimated the biological and physical contributions to the dynamic variations in O_2 and CO_2 in Hong Kong coastal waters. Coupled with the seasonal discharge from the Pearl River estuary, monsoons not only regulated the biological activities (e.g. NCP), but also variations in O_2 and CO_2 (Fig. 6). In the dry season, when strong vertical mixing resulted in light limitation due to the monsoon-induced downwelling, primary production (50–160 mmol C m^{-2} d^{-1}) was lower than community respiration ($\sim$160 mmol C m^{-2} d^{-1}). Hence, the heterotrophic status was associated with O_2 influxes and CO_2 effluxes. In the wet season, there was a contradictory observation of positive NCP (autotrophy) and CO_2 release and O_2 uptake in the mixed layer, which was likely due to the fact that the southwest monsoon-induced upwelling along with the lateral mixing brought low DO and CO_2-rich water to the surface which offset the DO increase and DIC decrease due to the high positive NCP. Despite the seasonal shifts between heterotrophy and autotrophy, Hong Kong waters were a CO_2 source to the atmosphere. Therefore, the trophic state does not always determine whether the water is a source or sink of CO_2 (Thomas et al., 2005; Chen, 2010), especially in dynamic coastal waters with anthropogenic forcing and complicated hydrodynamics.

Acknowledgements. This research was supported by grants from Hong Kong UGC AoE project (UGC AoE/P-04/04-1). We also acknowledge the support from the CAS/SAFEA International Partnership Program for Creative Research Teams (KZCX2-YW-T001), LMEB201001, NSFC Project 40676074 and Hong Kong RGC (HKUST6478/05M, HKUST6505/06M). We thank the staff in the Environmental Central Facility at HKUST for their excellent service. Thanks to Y. K. Tam for her assistance with general technical support.

Edited by: A. V. Borges

References

Barber, R. T., Marra, J., Bidigare, R. C., Codispoti, L. A., Halpern, D., Johnson, Z., Latasa, M., Goericke, R., and Smith, S. L.: Primary productivity and its regulation in the Arabian Sea during 1995, Deep-Sea Res. Pt. II, 48, 1127–1172, 2001.

Benson, B. B. and Krause, D.: The concentration and isotopic fractionation of oxygen dissolved in freshwater and seawater in equilibrium with the atmosphere, Limnol. Oceanogr., 29, 620–632, 1984.

Borges, A. V.: Present day carbon dioxide fluxes in the coastal ocean and possible feedbacks under global change, in: Oceans and the atmospheric carbon content, edited by: da Silva Duarte, P. M. and Santana Casiano, J. M., 47–77, 2011.

Borges, A. V. and Frankignoulle, M.: Distribution of surface carbon dioxide and air-sea exchange in the upwelling system off the Galician coast, Global Biogeochem. Cy., 16(2), 1020, doi:10.1029/2000GB001385, 2002.

Borges, A. V. and Gypens, N.: Carbonate chemistry in the coastal zone responds more strongly to eutrophication than to ocean acidification, Limnol. Oceanogr., 55, 346–353, 2010.

Borges, A., Delille, B., Schiettecatte, L., Gazeau, F., Abril, G., and Frankignoulle, M.: Gas transfer velocities of CO_2 in three European estuaries (Randers Fjord, Scheldt, and Thames), Limnol. Oceanogr., 49(5), 1630–1641, 2004.

Borges, A. V., Delille, B., and Frankignoulle, M.: Budgeting sinks and sources of CO_2 in the coastal ocean: Diversity of ecosystems counts, Geophys. Res. Lett., 32, L14601, doi:10.1029/2005GL023053, 2005.

Borges, A. V., Schiettecatte, L. S., Abril, G., Delille, B., and Gazeau, F.: Carbon dioxide in European coastal waters, Estuar. Coast. Shelf S., 70, 375–387, 2006.

Cai, W. and Wang, Y.: The chemistry, fluxes and sources of carbon dioxide in the estuarine waters of the Satilla and Altamaha Rivers, Georgia, Limnol. Oceanogr., 43, 657–668, 1998.

Cai, W., Dai, M., Wang, Y., Zhai, W., Huang, T., Chen, S., Zhang, F., Chen, Z., and Wang, Z.: The biogeochemistry of inorganic carbon and nutrients in the Pearl River estuary and the adjacent Northern South China Sea, Cont. Shelf Res., 24, 1301–1319, 2004.

Cai, W., Dai, M., and Wang, Y.: Air – sea exchange of carbon dioxide in ocean margins: a province-based synthesis, Geophys. Res. Lett., 33, L12603, doi:10.1029/2006GL026219, 2006.

Carrillo, C. J., Smith, R. C., and Karl, D. M.: Processes regulating oxygen and carbon dioxide in surface waters west of the Antarctic Peninsula, Mar. Chem., 84, 161–179, 2004.

Chen, C.: Cross-boundary exchanges of carbon and nitrogen in continental margins, in: Carbon and nutrient fluxes in continental margins: a global synthesis, edited by: Liu, K.-K., Atkinson, L., Quiñones, R., and Talaue-McManus, L., IGBP Book Series, Springer, Berlin, 561–574, 2010.

Chen, C. and Borges, A. V.: Reconciling opposing views on carbon cycling in the coastal ocean: Continental shelves as sinks and near-shore ecosystems as sources of atmospheric CO_2, Deep-Sea Res. Pt. II, 56, 578–590, 2009.

Chou, W., Gong, G., Sheu, D., Hung, C., and Tseng, T.: The surface distributions of carbon chemistry parameters in the East China Sea in summer 2007, J. Geophys. Res., 114, C07026, doi:10.1029/2008JC005128, 2009a.

Chou, W., Gong, G., Sheu, D., Jan, S., Hung, C., and Chen, C.: Reconciling the paradox that the heterotrophic waters of the East China Sea shelf act as a significant CO_2 sink during the summertime: Evidence and implications, Geophys. Res. Lett., 36, L15607, doi:10.1029/2009GL038475, 2009b.

Dai, M., Guo, X., Zhai, W., Yuan, L., Wang, B., Wang, L., Cai, P., Tang, T., and Cai, W.: Oxygen depletion in the upper reach of the Pearl River estuary during a very drought winter, Mar. Chem., 102, 159–169, 2006.

Diaz, R. J. and Rosenberg, R.: Spreading dead zones and consequences for marine ecosystems, Science, 321, 926–929, 2008.

Dickson, A. G. and Goyet, C.: Handbook of methods for the analysis of the various parameters of the carbon dioxide system in seawater, Version 2.0, Carbon dioxide information and analysis center, Oak Ridge, TN, 1994.

Dickson, M. L., Orchardo, J., Barber, R. T., Marra, J., McCarthy, J. J., and Sambrotto, R. N.: Production and respiration rates in the Arabian Sea during the 1995 Northeast and Southwest Monsoons, Deep-Sea Res. Pt. II, 48, 1199–1230, 2001.

Ducklow, H. W. and McCallister, S. L.: The sea, the Global Coastal Ocean, Chap. 9: The biogeochemistry of carbon dioxide in the coastal oceans, edited by: Robinson, A. R., Brink, K., and Rothschild, B. J., Harvard University Press, Cambridge, MA, 13, 269–315, 2004.

Gattuso, J. P., Frankignoulle, M., and Wollast, R.: Carbon and carbonate metabolism in coastal aquatic ecosystems, Annu. Rev. Ecol. Evol. S., 29, 405–434, 1998.

Gazeau, F., Middelburg, J. J., Loijens, M., Vanderborght, J. P., Pizay, M. D., and Gattuso, J.-P.: Planktonic primary production in estuaries: a comparison of the ^{14}C, O_2 and ^{18}O methods, Aquat. Microb. Ecol., 46, 95–106, 2007.

Goyet, C., Millero, F. J., Osullivan, D. W., Eischeid, G., McCue, S. J., and Bellerby, R. G. J.: Temporal variations of $p\mathrm{CO}_2$ in surface seawater of the Arabian Sea in 1995, Deep-Sea Res., 45, 609–623, 1998.

Guo, X., Cai, W.-J., Zhai, W., Dai, M., Wang, Y., and Chen, B.: Seasonal variations in the inorganic carbon system in the Pearl River (Zhujiang) estuary, Cont. Shelf Res., 28, 1424–1434, 2008.

Gypens, N., Borges, A. V., and Lancelot, C.: Effect of eutrophication on air-sea CO_2 fluxes in the coastal Southern North Sea: a model study of the past 50 years, Glob. Change Biol., 15(4), 1040–1056, 2009.

Harrison, P. J., Yin, K., Lee, J. H., Gan, J., and Liu, H.: Physical-biological coupling in the Pearl River Estuary, Cont. Shelf Res., 28, 1405–1415, 2008.

Ho, A. Y., Xu, J., Yin, K., Yuan, X., He, L., Jiang, Y., Lee, J. H., Anderson, D. M., and Harrison, P. J.: Seasonal and spatial dynamics of nutrients and phytoplankton biomass in Victoria Harbour and its vicinity before and after sewage abatement, Mar. Pollut. Bull., 57, 313–324, 2008.

Ho, A. Y., Xu, J., Yin, K., Jiang, Y., Yuan, X., He, L., Anderson, D. M., Lee, J. H., and Harrison, P. J.: Phytoplankton biomass and production in subtropical Hong Kong waters: influence of the Pearl River outflow, Estuar. Coast., 33, 170–181, 2010.

Ichimura, S., Parsons, T. R., Takahashi, M., and Seki, H.: A comparison of four methods for integrating ^{14}C-primary productivity measurements per unit area, J. Oceanogr., 36, 259–262, 1980.

Jassby, A. and Platt. T.: Mathematical formulation of relationship between photosynthesis and light for phytoplankton, Limnol. Oceanogr., 21, 540–547, 1976.

Knap, A., Michaels, A., Close, A., Ducklow, H., and Dickson, A.: Protocols for the Joint Global Ocean Flux Study (JGOFS) core measurement, Scientific Committee on Ocean Research, Manual and Guides 29, UNESCO, Paris, 11–122, 1994.

Kuang, C. and Lee, J. H.: Impact of reclamation and HATS Stage I on Victoria Harbour, Hong Kong, in: Proceedings of the Fourth International Symposium Environmental Hydraulics, edited by: Lee, J. H. and Lam, K. M., Balkema, Rotterdam, Netherlands, 1163–1168, 2004.

Laruelle, G. G., Dürr, H. H., Slomp, C. P., and Borges, A. V.: Evaluation of sinks and sources of CO_2 in the global coastal ocean using a spatially-explicit typology of estuaries and continental shelves, Geophys. Res. Lett., 37, L15607, doi:10.1029/2010GL043691, 2010.

Lee, J. H., Harrison, P. J., Kuang, C., and Yin, K.: Eutrophication dynamics in Hong Kong coastal waters: physical and biological interactions, in: The Environment in Asian Pacific Harbours, edited by: Wolanski, E., Springer, Netherlands, 187–206, 2006.

Lendt, R., Thomas, H., Hupe, A., and Ittekkot, V.: The response of the near surface carbonate system of the northwestern Arabian Sea to the SW monsoon and related biological forcing, J. Geophys. Res., 108, 3222, doi:10.1029/2000JC000771, 2003.

Longhurst, A., Sathyendranath, S., Platt, T., and Caverhill, C.: An estimate of global primary production in the ocean from satellite radiometer data, J. Plankton Res., 17, 1245–1271, 1995.

Mackenzie, F. T., Lerman, A., and Andersson, A. J.: Past and present of sediment and carbon biogeochemical cycling models, Biogeosciences, 1, 11–32, doi:10.5194/bg-1-11-2004, 2004.

Mintrop, L., Körtzinger, A., and Duinker, J. C.: The carbon dioxide system in the northwestern Indian Ocean during south-west monsoon, Mar. Chem., 64, 315–336, 1999.

Robinson, C. and Williams, P. J. L. B.: Respiration and its measurement in surface marine waters, in: Respiration in aquatic ecosystems, edited by: del Giorgio, P. A. and Williams, P. J. L. B., Oxford University Press, Oxford, 147–180, 2005.

Roy, R. N., Roy, L. N., Vogel, K. M., Porter-Moore, C., Pearson, T., Good, C. E., Millero, F. J., and Campbell, D. M.: The dissociation constants of carbonic acid in seawater at salinities 5 to 45 and temperatures 0 to 45 °C, Mar. Chem., 44, 249–267, 1993.

Sarma, V. V. S. S., Kumar, M. D., and Manerikar, M.: Emission of carbon dioxide from a tropical estuarine system, Goa, India, Geophys. Res. Lett., 28, 1239–1242, doi:10.1029/2000GL006114, 2001.

Shiah, F. and Ducklow, H. W.: Temperature regulation of heterotrophic bacterioplankton abundance, production, and specific growth rate in Chesapeake Bay, Limnol. Oceanogr., 39, 1243–1258, 1994.

Takahashi, T., Sutherland, S. C., Sweeney, C., Poisson, A., Metzl, N., Tilbrook, B., Bates, N., Wanninkhof, R., Feely, R. A., Sabine, C., Olafsson, J., and Nojiri, Y.: Global sea-air CO_2 flux based on climatological surface ocean $p\mathrm{CO_2}$, and seasonal biological and temperature effects, Deep-Sea Res., 49, 1601–1622, 2002.

Therriault, J. C. and Levasseur, M.: Control of phytoplankton production in the Lower St Lawrence Estuary: Light and freshwater runoff, Nature Canada, 112, 77–96, 1985.

Thomas, H., Bozec, Y., de Baar, H. J. W., Elkalay, K., Frankignoulle, M., Schiettecatte, L.-S., Kattner, G., and Borges, A. V.: The carbon budget of the North Sea, Biogeosciences, 2, 87–96, doi:10.5194/bg-2-87-2005, 2005.

Thomas, H., Schiettecatte, L.-S., Suykens, K., Koné, Y. J. M., Shadwick, E. H., Prowe, A. E. F., Bozec, Y., de Baar, H. J. W., and Borges, A. V.: Enhanced ocean carbon storage from anaerobic alkalinity generation in coastal sediments, Biogeosciences, 6, 267–274, doi:10.5194/bg-6-267-2009, 2009.

Wanninkhof, R.: Relationship between wind speed and gas exchange over the ocean, J. Geophys. Res., 97, 7373–7382, 1992.

Weiss, R. F.: Carbon dioxide in water and seawater: the solubility of a non-ideal gas, Mar. Chem., 2, 203–215, 1974.

Yin, K.: Monsoonal influence on seasonal variations in nutrients and phytoplankton biomass in coastal waters of Hong Kong in the vicinity of the Pearl River Estuary, Mar. Ecol.-Prog. Ser., 245, 111–122, 2002.

Yin, K.: Influences of monsoons and oceanographic processes on red tides in Hong Kong waters, Mar. Ecol.-Prog. Ser., 262, 27–41, 2003.

Yin, K. and Harrison, P. J.: Influence of the Pearl River estuary and vertical mixing in Victoria Harbor on water quality in relation to eutrophication impacts in Hong Kong waters, Mar. Pollut. Bull., 54, 646–656, 2007.

Yin, K., Lin, Z., and Ke, Z.: Temporal and spatial distribution of dissolved oxygen in the Pearl River Estuary and adjacent coastal waters, Cont. Shelf Res., 24, 1935–1948, 2004.

Yuan, X., Yin, K., Harrison, P. J., Cai, W., He, L., and Xu, J.: Bacterial production and respiration in sub-tropical Hong Kong waters: influence of the Pearl River discharge and sewage impacts, Aquat. Microb. Ecol., 58, 167–179, 2010a.

Yuan, X., Yin, K., Harrison, P. J., He, L., and Xu, J.: Variations in apparent oxygen utilization and effects of P addition on bacterial respiration in subtropical Hong Kong waters, Estuar. Coast., doi:10.1007/s12237-010-9329-7, in press, 2010b.

Zhai, W., Dai, M., Cai, W., Wang, Y., and Wang, Z.: High partial pressure of CO_2 and its maintaining mechanism in a subtropical estuary: the Pearl River estuary, China, Mar. Chem., 93, 21–32, 2005a.

Zhai, W., Dai, M., Cai, W., Wang, Y., and Hong, H.: The partial pressure of carbon dioxide and air-sea fluxes in the northern South China Sea in spring, summer and autumn, Mar. Chem., 96, 87–97, 2005b.

Zhai, W., Dai, M., and Cai, W.: Coupling of surface $p\mathrm{CO_2}$ and dissolved oxygen in the northern South China Sea: impacts of contrasting coastal processes, Biogeosciences, 6, 2589–2598, doi:10.5194/bg-6-2589-2009, 2009.

Zhao, H.: Evolution of the Pearl River Estuary, Ocean Press, Beijing, 1–110, 1990.